International Edition: DOI: 10.1002/anie.201712296
German Edition: DOI: 10.1002/ange.201712296

Soft Landing of Ions

From Isolated Ions to Multilayer Functional Materials Using Ion Soft Landing

Julia Laskin, Grant E. Johnson,* Jonas Warneke, and Venkateshkumar Prabhakaran*

Keywords:
3D layered materials ·
charge retention ·
ion soft landing ·
mesoscale aggregates ·
self-organizing
layers

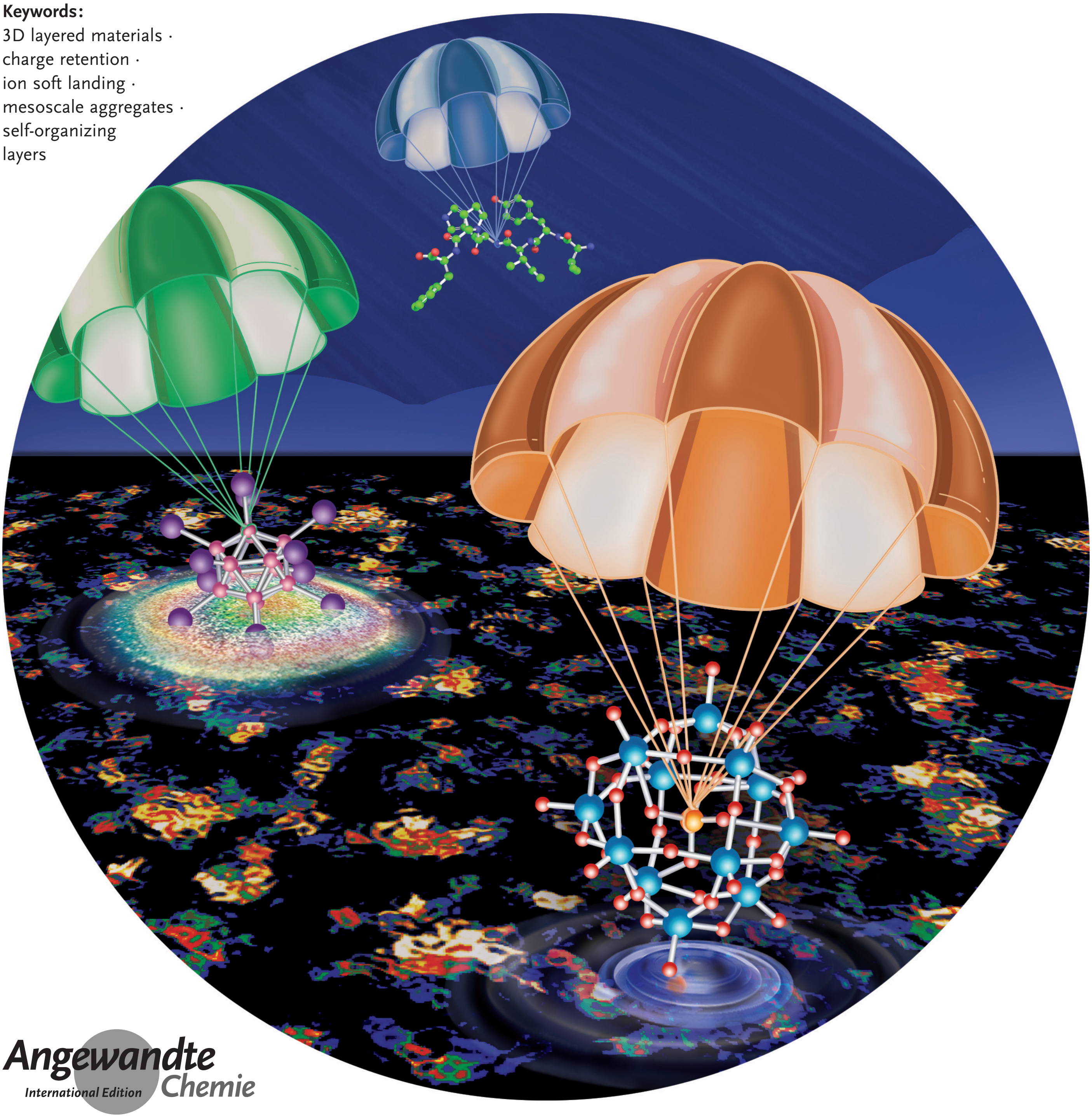

The ability to deposit intact polyatomic ions with well-defined composition, charge state, and kinetic energy onto surfaces makes preparative mass spectrometry, also called ion soft landing, particularly attractive for preparing uniform molecular and ionic layers. Early studies characterized the structures, charge states, and reactivity of sparsely distributed soft-landed species. The recent development of high-flux ionization sources has opened up new opportunities for the precisely controlled preparation of both two-dimensional structures and three-dimensional multilayer architectures by ion soft landing. The deposition of large numbers of ions onto supports led to previously unknown phenomena being uncovered, thereby opening several exciting research directions. Furthermore, faster ion deposition has enabled fabrication of novel functional devices. This Review discusses important phenomena and highlights key developments pertaining to the preparation of well-defined interfaces for studies in energy storage, catalysis, soft materials, and biology.

From the Contents

1. Introduction

Mass spectrometry, commonly used as a powerful tool for a variety of analytical applications, is ideally suited for the preparation of charged molecules with well-defined compositions and charge states. This capability prompted the development of preparative mass spectrometry, in which mass- and charge-selected ions are deposited onto surfaces.[1–10] Molecular ions are typically delivered to surfaces with kinetic energies in the hyperthermal range (1–100 eV). This gentle deposition process, called ion soft landing, is analogous to molecular beam epitaxy but uses charged species instead of neutral molecules. Although ion currents are substantially lower than typical fluxes of neutral molecules used in molecular beam epitaxy, ion soft landing provides access to a broad range of both stable and chemically labile charged species, from small atomic ions to large protein complexes in the megadalton mass range. Patterning of the ion beam and control of the ion kinetic energy are important capabilities that further distinguish ion soft landing from other deposition techniques. Furthermore, gas-phase ion chemistry may be used to generate species that cannot be synthesized in solution, which opens up opportunities for examining the properties of materials prepared from building blocks that are unavailable by traditional chemistry methods.

Since its introduction by the Cooks group in 1977,[11] ion soft landing has been used predominately for studying uniformly distributed isolated ions on surfaces. These studies provided a detailed understanding of the physical and chemical phenomena accompanying ion deposition, including the structure and reactivity of isolated ions on surfaces, charge retention, covalent-bond formation between ions and functional groups on the surface, secondary structure, and biological activity of soft-landed peptides and proteins. The progress in this area of ion soft landing research has been extensively reviewed[1–10] and will not be discussed here. Instead, this Review will focus on an emerging and promising area in this field, in which mass spectrometry is being used to prepare aggregates and multilayer architectures. Recent developments in ion soft landing instrumentation have resulted in at least an order of magnitude increase in the achievable ion current, which prompted the transition from studying isolated species to more complex multilayer materials. The ability to conduct layer-by-layer ion deposition, which will open up new applications using beams of mass-selected complex ions, relies on understanding the physicochemical processes accompanying ion–surface collisions. For example, soft-landed ions often retain their charge and a substantial potential may be created on the surface upon the accumulation of ions.[3] Understanding charge retention and processes that stabilize multilayered ion-based architectures is critically important for controlling high-flux ion-deposition processes.

---

[*] Prof. J. Laskin
Department of Chemistry, Purdue University
West Lafayette, IN 47907 (USA)
E-mail: jlaskin@purdue.edu
Dr. G. E. Johnson, Dr. J. Warneke, Dr. V. Prabhakaran
Physical Sciences Division
Pacific Northwest National Laboratory
Richland WA, 99352 (USA)
E-mail: grant.johnson@pnnl.gov

The ORCID identification number(s) for the author(s) of this article can be found under: https://doi.org/10.1002/anie.201712296.

This Review is organized as follows. First, we discuss recent developments in ion soft landing instrumentation. Next, we describe a two-plate capacitor model, which helps rationalize the accumulation of charged species of the same polarity on surfaces. Finally, we present several examples of high-flux ion deposition for preparing electrochemical energy storage devices, catalytically active cluster assemblies, self-organizing anion-based layers, and arrangements of large molecules for applications in soft materials and biology.

2. Advances in Soft Landing Instrumentation

Ion soft landing experiments typically utilize custom-designed vacuum-based instruments in which an ionization source is coupled to a mass filter that delivers mass-selected ions to the deposition surface.[1,2,5,6] Although a broad range of ionization techniques and mass analyzers may be used for ion deposition, continuous ionization sources and mass-filtering devices provide the highest possible ion fluxes and are, therefore, preferred over pulsed systems with lower duty cycles. Electrospray ionization (ESI) is one of the most widely used techniques for ion deposition, with or without mass selection.[12] ESI produces fairly bright beams of ions present in solution or polar molecules that ionize by formation of an adduct or proton detachment. Alternatively, a nonthermal magnetron sputtering source combined with gas aggregation has been used to generate charged clusters and nanoparticles of different size, composition, and structure that cannot be synthesized in solution.[13] These ionization sources are often coupled to a quadrupole mass analyzer, which is used as a mass-filtering device. For a detailed description of soft landing instrumentation, the readers are referred to comprehensive reviews.[1,2,5,6] In the following, we highlight the most recent developments, which have substantially enhanced the achievable ion currents and opened up several exciting research directions in this field.

Recent advances in ESI-based soft landing instrumentation focused on the improved transfer of charged droplets from the emitter into the vacuum system of a mass spectrometer and more efficient desolvation of the droplets at the atmospheric interface. Ion currents in the range of 1 to 10 nA have been achieved either by increasing the inner diameter[14] or precisely shaping the heated inlet of the instrument.[15] The implementation of the dual ion funnel interface enabled the instrument to be operated with a higher gas load in the vacuum, thereby resulting in an almost tenfold increase in the ion current. The substantial increase in ion current is critical to the preparation of 2D molecular structures and 3D multilayer architectures.

Notable developments have occurred in physical cluster/nanoparticle synthesis techniques based on sputtering and gas aggregation. In particular, a new multi-magnetron source was introduced which incorporates three separate metal targets that may be placed at controlled locations within one aggregation region.[16] A supersonic cluster beam apparatus was also developed and used for the rapid prototyping of cluster-based electrical components.[17] In addition, high-

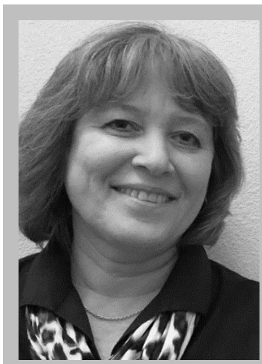

Julia Laskin received her Master's degree in Physics from the Polytechnical Institute, St. Petersburg, Russia (1990) and PhD in Physical Chemistry from the Hebrew University of Jerusalem (1998). After postdoctoral appointments at the University of Delaware (1998-99) and Pacific Northwest National Laboratory (PNNL; 2000-02), she became a research scientist at PNNL (2002–2017). In 2017, she joined the Department of Chemistry at Purdue University as the William F. and Patty J. Miller Professor. Her research is focused on selective surface modification using ion beams and developing new approaches for imaging biological materials.

Jonas Warneke received his BS in Chemistry in 2009, his MS in Material Science in 2011, and his PhD in Physical Chemistry in 2015 from the University of Bremen in Germany. Since 2016 he has been a Feodor Lynen Fellow of the Alexander von Humboldt Foundation at PNNL. His research focuses on the fundamental understanding of highly stable boron cluster anions and their use in material preparation through ion soft landing.

Grant Johnson received his BS in chemistry in 2002 from the University of Delaware and PhD in chemistry in 2009 from Pennsylvania State University. From 2010 to 2012 he worked at PNNL as the inaugural Linus Pauling Postdoctoral Fellow. In 2015 he received the Ronald L. Brodzinski Award for Early Career Exceptional Achievement at PNNL. He leads the Separations program at PNNL, which is focused on developing a fundamental understanding of structure–function relationships to support the design and synthesis of tailored materials for improved separations.

Venkateshkumar Prabhakaran received his BS from the Central Electrochemical Research Institute, India, in 2009 and his PhD in Chemical Engineering from the Illinois Institute of Technology in 2014. Following postdoctoral research at PNNL (2014–2017), he became a research scientist. In 2017, he was awarded the EMSL M.T. Thomas Award for his outstanding postdoctoral work. His research focuses on the preparation of novel electrode materials by soft and reactive landing of ions as well as in situ and operando techniques of electrochemical processes at well-defined electrode–electrolyte interfaces.

power impulse magnetron sputtering was shown to produce large currents of mass-selected metal clusters.[18] A recently developed "Matrix Assembly Cluster Source" (MACS) produces several nanoamperes of equivalent current, which corresponds to the combined flux of neutral and charged nanoclusters.[19] In this source, the clusters are formed by condensation of metal atoms and ions inside a cold (ca. 15 K) matrix.[20] The process is initiated by bombarding the matrix with a high-energy ion beam to promote atomic collisions and sputtering of clusters generated through a collision cascade into the gas phase. The variation in the diameter of the clusters is about 10% without mass selection.

The most probable cluster size is determined by the temperature of the matrix, primary ion beam parameters, and metal concentration in the matrix. Furthermore, colloidal suspensions may be produced by depositing clusters onto water-soluble polymer films and subsequently transferring the polymer-encapsulated clusters into solution by sonication.[21] This approach should be, in principle, scalable to milliamperes of ion current, which will result in an unprecedented rate of cluster deposition.

3. Ambient Soft Landing

Certain advantages of soft landing of mass-selected ions in a vacuum may be reproduced in the laboratory with substantially reduced equipment and expense by using an alternative approach called ambient ion soft landing.[22] This simplified soft landing technique involves deposition of polyatomic ions from air onto a surface at a selected location at atmospheric pressure. As shown in Figure 1, charged droplets generated by ESI are passed pneumatically through a heated drying tube to ensure efficient ion desolvation. Ion polarity (+/−) is then selected using electrostatic deflectors, and the desolvated polarity-selected ions are soft landed onto a chosen surface in open air. In contrast to traditional soft landing experiments in a vacuum, where ions are selected by their mass-to-charge ratio, here the ions to be deposited are selected through the choice of a chemical compound that produces mainly one ionic species in a given charge state during ESI.[22] This more accessible ion-deposition approach has a number of advantages compared to conventional solution-based preparation methods, such as drop casting and spin coating, since it eliminates neutral molecules and counterions from the surface.

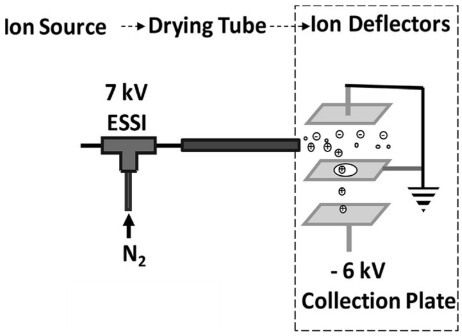

Figure 1. Schematic diagram of the electrospray emitter, drying tube, and electrostatic deflectors used for ion soft landing under ambient conditions. Reproduced from Ref. [23] with permission. Copyright 2011, American Chemical Society.

Recently, it was demonstrated that ESI of solutions of metal salts followed by heating in air transforms salt clusters into naked ionic metal clusters. In essence, the heated, coiled, drying loop serves to release the counterions while generating naked anionic or cationic metal clusters.[23] This development has important implications for the preparation of metal clusters and nanoparticles for catalysts and optical sensors, including species that are not readily synthesized in solution. For example, ambient ion beams combined with nonconductive masks were used to prepare structured patterns of Ag nanoparticles for surface-enhanced Raman spectroscopy (SERS) with substantial enhancement factors of up to 10^8.[24] In another study, soft landing was used to create 2D nano-networks of molecules on graphite under ambient conditions. This resulted in a close-packing structure instead of the more typical unorganized clusters formed by solution deposition.[25] An interesting aspect of this study was the detection of positively charged species, thus indicating the retention of charge on the modified surfaces. In a recent study, dandelion-like CuO-Ag hybrid nanostructures were prepared on surfaces through electric field induction of electrosprayed Ag ions and clusters.[26] The process involved the production of charged Ag clusters by ionization at atmospheric pressure followed by soft landing and electrostatically induced self-assembly of the ions on the tips of CuO nanowires. Ambient soft landing was recently used to prepare protein chips for analytical mass spectrometry.[27] The chips were used for the development of bioanalytical assays based on the interaction between the immobilized protein and the sampled analyte directly on the chip. Potential future developments for ambient soft landing as an approach to surface modification include the incorporation of electrode devices capable of focusing, reacting, and separating ions in the open air, thereby achieving some ion manipulations similar to those conducted routinely in vacuum.[28] New hydrodynamic interfaces to ensure complete desolvation of ions in droplets produced by electrospray will also increase the throughput and decrease the contamination associated with soft landing in benchtop instruments.[29]

Ambient soft landing benefits from the accelerated reaction kinetics occurring in desolvating microdroplets. For example, this approach was employed to derivatize biomolecules through the efficient formation of amide bonds between amines and carboxylic acids in charged microdroplets.[30] The derivatized species self-assembled on bare gold surfaces through the formation of Au−S bonds. The interaction of charged droplets containing organic compounds with solid surfaces was also shown to be more efficient than the equivalent reaction performed in bulk solution.[31] The increased reactivity was attributed to evaporation of the solvent, which results in dramatic increases in the concentration and pH value in the droplets. In another study, it was observed that chemical reactions within organic layers and at interfaces of organic films and an aqueous phase or the atmosphere often exhibit markedly different reactivity to that shown by the same compounds in bulk solutions.[32] In summary, ambient soft landing is a versatile and cost-effective technique for modifying surfaces with complex ions that produce primarily a single ion through ESI. Recent studies indicate promising uses of this method in the synthesis of clusters and nanoparticles for catalysis and spectroscopy, highly efficient and selective droplet reactions, and bioanalytical applications.

4. Charge Retention and the Capacitor Model

Since being discovered by the Cooks group in 1997,[33] charge retention by soft-landed ions on surfaces coated with insulating layers has been extensively investigated.[34,35] It has been demonstrated that the efficiency of charge loss by deposited ions is affected by the properties of the surface, mode of ionization of the projectile ion, and coverage. Detailed discussion of this topic may be found in several recent reviews.[2,5,7,8] Briefly, efficient charge retention, which is largely independent of the properties of the surface and ion coverage, was observed for stable anions.[36,37] This observation was attributed to the high energy barrier for the detachment of an electron from the anion for either partial loss of charge or complete neutralization. In contrast, cations undergo more efficient charge reduction when soft landed onto thin insulating self-assembled monolayers (SAMs).[35,38,39] The tunneling of electrons from the underlying metal surface through the insulating layer is the key factor affecting the charge reduction of native cations. Electron tunneling rates are affected by the properties of the SAM and may be controlled by tailoring the interface dipoles of the layers facing the ion beam. Furthermore, the accumulation of ions on top of the layer generates an electric field gradient across the SAM, which facilitates electron tunneling.[39] As a result, charge retention by native cations is affected by ion coverage. Finally, protonated species soft landed onto SAMs were found to undergo proton abstraction, which was least efficient on fluorinated and most efficient on carboxy-terminated SAMs.[35]

Regardless of the mechanism of charge reduction, partial or complete retention of charge by soft-landed ions raises a concern that a substantial potential may build up on the substrates and block the ion beam from reaching the surface. However, experimentally, a stable current is measured on the conductive substrate during deposition even if charge is retained by the soft-landed ions. The efficient deposition of ions onto a layer of species with the same charge already present on the surface seems counterintuitive at first, but may be rationalized using a simplified parallel plate capacitor model. According to this model, the presence of permanent charges (the deposited ions) near the metal surface above a thin insulating layer such as a SAM induces a displacement of the electrons in the conductor. The conductive substrate, if grounded, accumulates a charge opposite to that of the deposited ions, which results in an electric field that may be described by the model of image/mirror charges (Figure 2a). This preserves the overall neutrality of the system. If

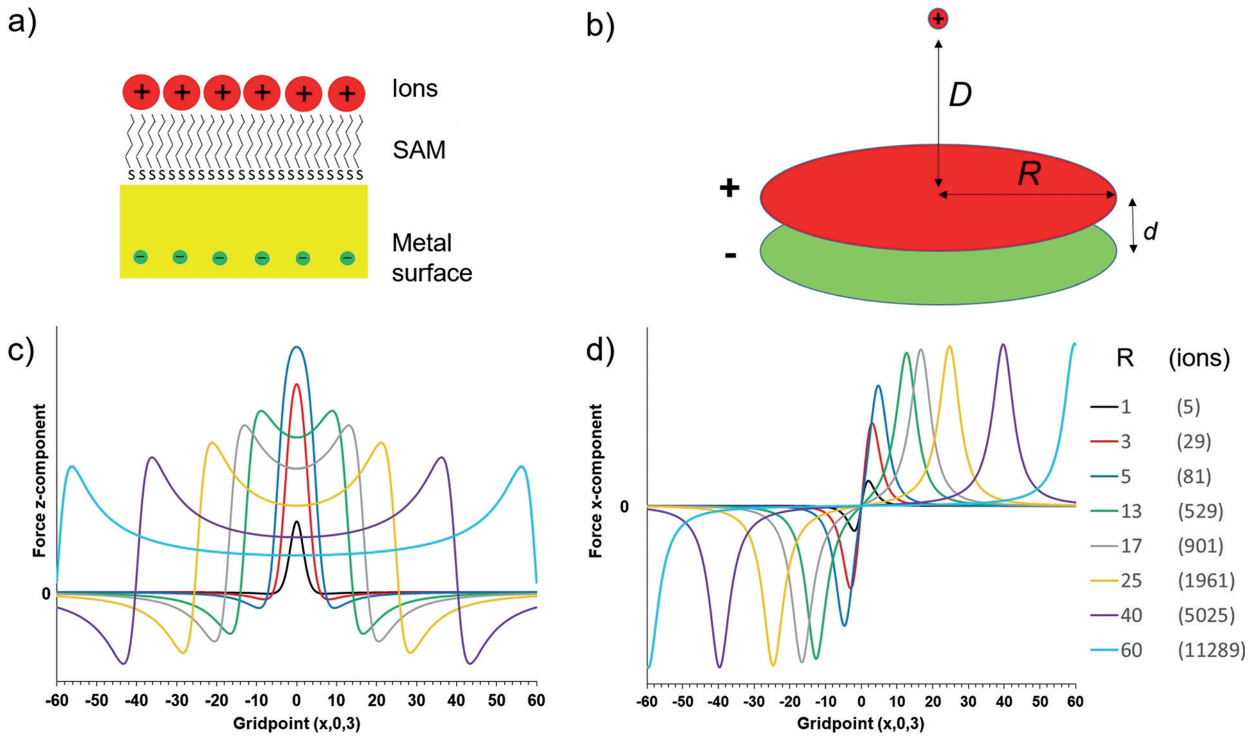

Figure 2. a) Representation of the parallel plate capacitor model in ion soft landing. The field of the grounded conductive substrate may be modeled by point charges that are located at the positions of the ions mirrored on the conductive surface. b) Schematic diagram of the physical model described in Equation (1). c) *z* component and d) *x* component of the force on a point charge at different positions over an array of charges. See text for details.

the layer of soft-landed ions and mirror charges is approximated by uniformly charged round plates with radius R separated by a distance d (Figure 2b), the force F on an ion approaching the center of the plate at distance D may be expressed using Equation (1).[3]

$$F = \frac{Z^2}{2\varepsilon_0}\frac{N_{\text{ions}}}{A}\left(-\frac{D}{\sqrt{R^2+D^2}}+\frac{D+d}{\sqrt{R^2+(D+d)^2}}\right) \qquad (1)$$

From Equation (1), it follows that for a large capacitor (very large R), the electric field above the center of the plates is extremely small and vanishes for infinitely large plates. This approximation has been used previously to explain stable deposition currents observed throughout the continuous accumulation of charges of the same polarity on surfaces.[3] However, the infinite parallel plate capacitor approximation does not account for side effects at the borders of the plates. To understand how the electric field develops over a monolayer of charges with increasing radius R at different positions, we established the following model: The deposited ions are represented as a two-dimensional array of evenly distributed point charges located at grid points $(x,y,0)$ within a given radius R from (0,0,0). The radius of the array is varied by changing the number of point charges while keeping the density of the charged species constant. The same array of point charges with negative values is located at $(x,y,-1)$ to represent the mirror charges in the underlying conductive surface. The electric field above the two-dimensional array of deposited ions and its mirror charge was calculated by adding up the individual contributions of all the charges. In Figure 2c, the z-component (repulsive force) that acts on an approaching ion three grid units above the layer along a line $(x,0,3)$ is plotted for different radii R. Figure 2d represents the corresponding x-component of the force. For small radii R (small number of ions), the repulsive force in the middle initially increases with R but, with the addition of further ions, then drops. It follows that ions approaching the middle region of an extended layer of deposited ions are affected little by electric fields. In contrast, the lateral component of the field (Figure 2d) close to the edge of the array increases gradually at small radii and remains almost constant at larger radii. Consequently, slow ions approaching the borders may be relegated to the outer positions of the layer. Since the experimental deposition profile is expected to be Gaussian shaped, less pronounced border effects may be expected than in this idealized array.

As the charge density on the surface increases, the potential between the metal substrate and the layer of soft-landed ions increases, which may, in the case of high-coverage depositions, result in a breakdown of the capacitor through electron tunneling and neutralization of the deposited ions on top of the SAM. One example of capacitor breakdown was reported for ligated gold cluster cations deposited at fairly high coverage onto a fluorinated self-assembled monolayer (FSAM) surface.[39] In contrast, recent multilayer depositions of electronically stable anions did not result in considerable neutralization.[36,37] Investigations pointed to preservation of the anionic charge state on the surfaces. Characterization of these layers showed that hydrocarbons (primarily phthalates) from the instrument background accumulated together with the deposited anions, which helped stabilize the layers. These layers with a high coverage of anions exhibited remarkable properties as interfaces for supercapacitors[40] or self-organizing layers,[41] as will be discussed in the following sections. Based on the high density of anions that must be present in such multilayer materials we propose that the layer is not electrostatically stabilized by the image charges alone. Instead, other stabilization mechanisms including coadsorption of neutral molecules and their partial oxidation must also be taken into account. Understanding these processes at a fundamental molecular level is an important challenge facing research on ion soft landing at high coverage.

5. Designing Electrode–Electrolyte Interfaces Using Ion Soft Landing

Electrochemical interfaces are an integral part of energy conversion and storage technologies.[42,43] Charge transfer, migration under electric fields, and ionic diffusion are primary interfacial processes, which take place at operating electrode–electrolyte interfaces (EEIs).[43,44] The stability of solid EEIs is dependent on the efficiency of these interfacial processes. Numerous degradation mechanisms in solid EEI-based electrochemical systems have been reported in the literature. Examples include agglomeration and decomposition of redox-active species on electrode surfaces (supercapacitors, batteries), catalyst dissolution, and generation of undesired parasitic side products during the oxygen reduction reaction (ORR) at electrodes in polymer electrolyte membrane fuel cells (PEMFCs).[45] A fundamental understanding of relevant phenomena, such as dynamic changes in the local molecular and electronic structures, chemical reactivity of species bound to electrode surfaces, and intrinsic properties of electroactive moieties at operating EEI, is essential to the development of efficient and sustainable solid-state energy technologies.[46]

Recent studies demonstrated that ion soft landing is ideally suited for designing well-defined EEIs through the deposition of mass-selected electroactive ions onto electrodes. This capability is important to obtaining a detailed understanding of molecular-level processes on electrodes without the complications of side reactions, contaminants, and electrochemically inactive counterions.[8] For example, understanding the effect of counterions on the performance of redox supercapacitors may be achieved through mass-selected deposition of electroactive ions such as multielectron redox-active polyoxometalate (POM) anions (Figure 3a).[47] The elimination of strongly coordinating counterions from EEIs prepared by the soft landing of molybdenum POM anions ($[PMo_{12}O_{40}]^{3-}$) resulted in a substantial decrease in the interfacial charge-transfer resistance, which enhanced the performance and long-term stability of a redox supercapacitor.[47] Specifically, more than a 30% increase in the energy storage capacity of carbon nanotube electrodes (CNTs) was achieved by depositing only 50 ng (0.2 wt%) of pure POM anions uniformly on top of the electrode. In contrast, more than 100 ng of POM was necessary to achieve a comparable capacitance as electrodes prepared by ambient electrospray

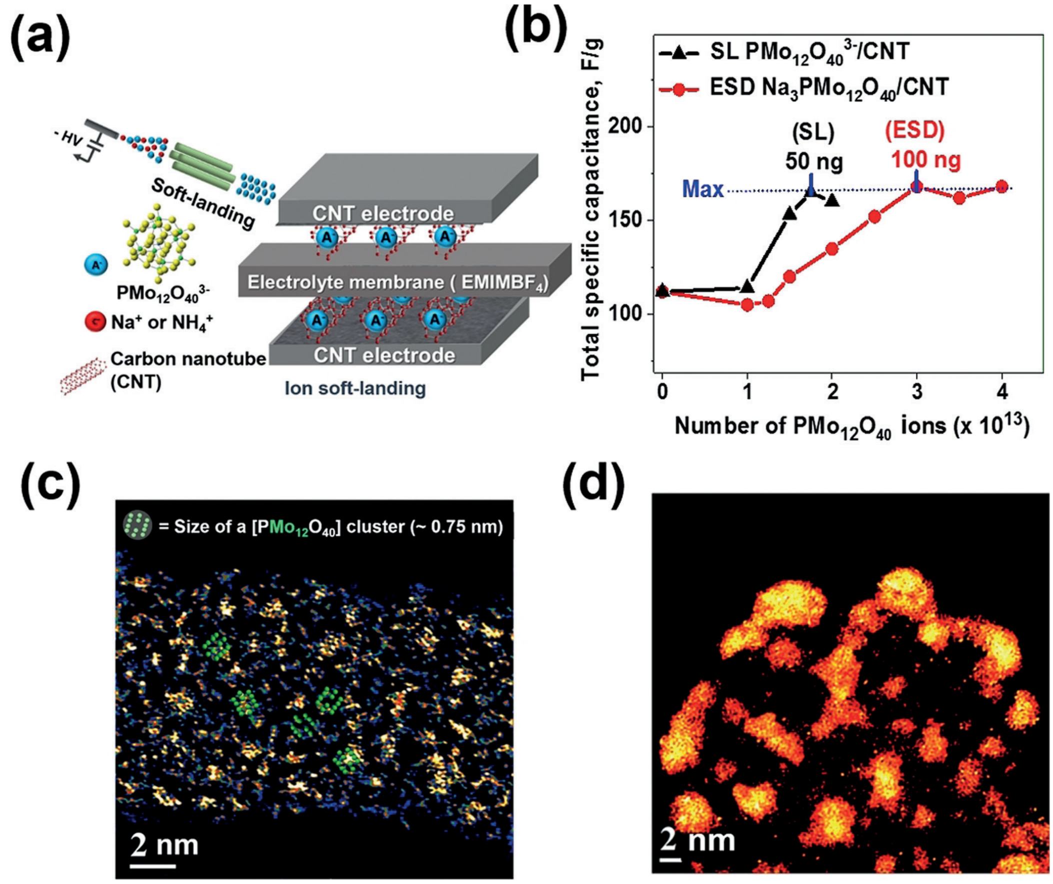

Figure 3. a) Schematic representation of an EEI prepared using ion soft landing of $[PMo_{12}O_{40}]^{3-}$ onto CNT electrodes that do not contain strongly coordinating cations as counterions. b) The total specific capacitance of electrodes prepared by soft landing (SL) and ambient electrospray deposition (ESD) at different loadings of $[PMo_{12}O_{40}]$ ions. c) Atomically resolved STEM images of the uniformly distributed soft-landed $[PMo_{12}O_{40}]^{3-}$ ions. d) STEM images of the surface after ESD showing the formation of aggregates of $[PMo_{12}O_{40}]$ as a consequence of the presence of counterions. Reproduced from Ref. [48] with permission. Copyright 2016, Nature Publishing Group.

deposition (ESD; Figure 3b). Furthermore, the long-term stability of the ESD electrodes was inferior to the ones prepared using mass-selected ion soft landing. Scanning transmission electron microscopy (STEM) images revealed a uniform distribution of individual POM anions on electrodes prepared by ion soft landing (Figure 3c) and substantial agglomeration of POM on electrodes prepared by ESD, which affects their performance. Similarly, a remarkable increase in the photoelectrochemical activity of metal oxide electrodes was observed after deposition of a sub-monolayer amount of mass-selected Ti nanoclusters.[48] These proof-of-principle studies demonstrate the power of soft landing for the preparation of high-efficiency technologically relevant EEIs and provide the first mechanistic insights into relevant processes occurring at EEIs.

In situ characterization of processes at solid EEIs prepared using ion soft landing will facilitate the rational design of improved functional interfaces for solid-state electrochemical devices. A solid-state in situ electrochemical cell was developed to address this challenge. The cell is composed of a screen-printed electrode and a specially designed thin nanoporous membrane in which an ionic liquid (IL) serves as a solid-state electrolyte (Figure 4a). Two different membranes were developed to enable the characterization of both the intrinsic redox and reactive processes at EEIs. The nanoporous membranes were found to have excellent mass-transport properties, comparable to those of liquid electrolytes, and to be stable in vacuum and different reactive gaseous environments (Figures 4a,b).[49] Soft landing enables precise control over the stoichiometry and distribution of electroactive species at EEIs (Figures 4c,d). The thin nanoporous membrane mimics solid electrolytes used in numerous devices, which facilitates understanding of electrochemical processes occurring on technologically relevant EEIs.

The redox activity of POM anions was examined using an electrochemical cell containing an aprotic IL membrane (Figure 4c). In situ cyclic voltammetry (CV) measurements showed multielectron redox processes for $[PMo_{12}O_{40}]^{3-}$ (Figure 4e) and its doubly charged protonated analogue $[HPMo_{12}O_{40}]^{2-}$. The different response of the two charge states of POM anions in CV experiments was attributed to inhibited electron transfer to the POM as a result of the presence of H^+ ions in $[HPMo_{12}O_{40}]^{2-}$. Additionally, two complementary fragment ions of $[PMo_{12}O_{40}]^{3-}$, namely $[Mo_7O_{22}]^{2-}$ and $[PMo_5O_{18}]^-$, were produced in the gas phase through collision-induced dissociation (CID) and deposited onto the aprotic cell. CV analysis of the fragments revealed a synergistic interaction between $[Mo_7O_{22}]^{2-}$ and $[PMo_5O_{18}]^-$

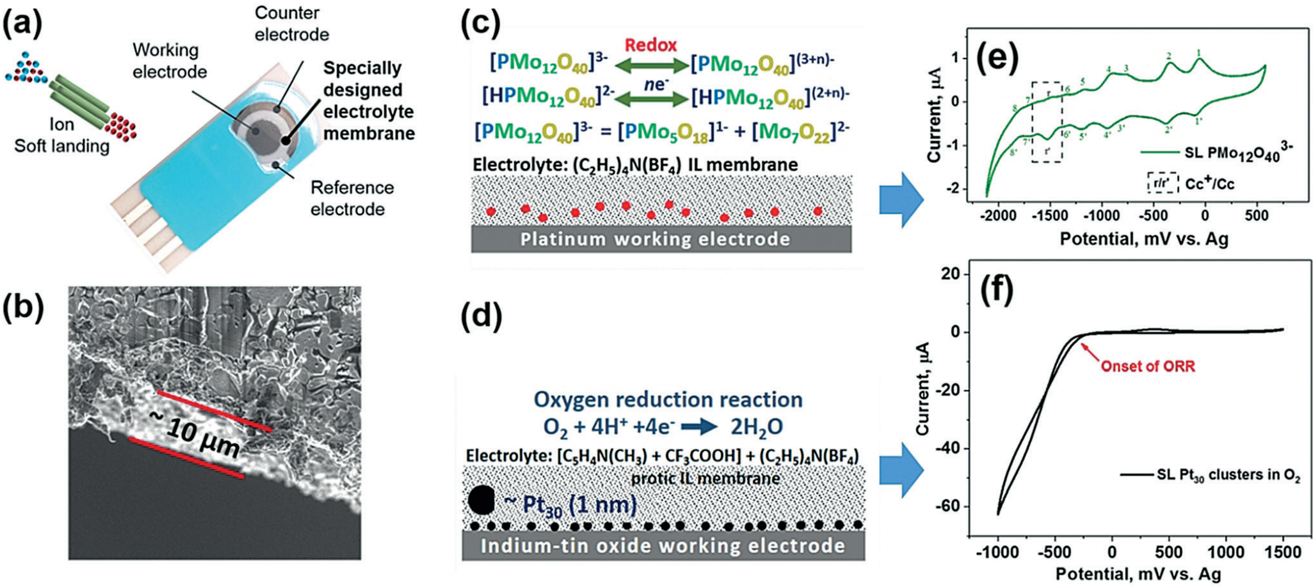

Figure 4. a) Schematic drawing of the in situ solid-state electrochemical cell prepared using ion soft landing. b) Scanning electron micrograph of the nanoporous thin ionic liquid membrane. c,d) Schematic representation of redox and electrochemical reactions, respectively, studied using the in situ cell. e) Representative cyclic voltammogram of soft-landed $[PMo_{12}O_{40}]^{3-}$ showing multiple well-resolved redox steps obtained using the in situ aprotic IL cell represented in (c); Cc^+/Cc = cobaltacene redox couple, used as an internal reference. f) Representative cyclic voltammograms of soft-landed Pt_{30} clusters showing significant oxygen reduction activity obtained using the in situ protic IL cell represented in (d). Reproduced from Ref. [49] with permission. Copyright 2016, National Academy of Sciences.

and subsequent electron transfer within the cluster, which is collectively responsible for the redox activity of the intact $[PMo_{12}O_{40}]^{3-}$ cluster. These experiments highlight the power of ion soft landing combined with the in situ electrochemical cell for understanding the contribution of individual building blocks to the multielectron redox activity of deposited electroactive species.

Electrochemical reactions may also be explored using the in situ electrochemical cell with an appropriate IL membrane. For example, the reduction of oxygen on bare Pt clusters (e.g. Pt_{30}) produced by magnetron sputtering and gas aggregation was examined using a protic IL (Figure 4 d). This protic IL cell is stable in vacuum during ion deposition and serves as the source of protons during the electrochemical reduction of oxygen. The activity of Pt_{30} clusters (Figure 4 f) was comparable to conventional Pt-based electrodes, which confirms the reliability of this in situ cell for studying electrochemical reactions of electroactive clusters.

In summary, the solid-state thin-film in situ electrochemical cell combined with ion soft landing enables electrochemical characterization of well-defined uniformly distributed ions at EEIs. This capability will facilitate molecular-level understanding of key electron- and ion-transfer processes at technologically relevant nanoporous EEIs during electrocatalytic operation. In general, the approach of coupling in situ electrochemical techniques with soft landing opens up new opportunities to probe electrode kinetics of well-defined ions at operating solid–electrolyte model interfaces. This has strong implications for research in catalysis and energy technologies.

6. Catalytic Particles—From Isolated Ions to Particle Assemblies

Ion soft landing has been used for over 30 years to prepare well-defined model systems of supported clusters for fundamental studies in heterogeneous catalysis.[50,51] Several review articles describing this work are available in the literature.[4,7,10,52–54] Briefly, Heiz et al. demonstrated the soft landing of mass-selected metal cluster ions, produced through laser vaporization and gas condensation, onto thin metal oxide films.[55] Subsequent surface characterization using infrared spectroscopy and temperature-programmed desorption combined with theoretical calculations provided insights into the role of cluster size, surface defects, and interfacial electron transfer on catalytic reactions promoted by supported clusters.[56] Later studies established a correlation between the oxidation activity of size-selected Pd_n clusters supported on TiO_2 and the binding energies of their 3d electrons, as measured by X-ray photoelectron spectroscopy.[57] Characterization of the size-dependent catalytic activity of Pd_n clusters supported on graphite revealed a substantial increase in turnover rates with decreasing cluster size.[58] In addition to activity, the selectivity of reactions toward desired products is another important metric of overall catalytic performance that may vary with cluster size. For example, size-selected Pt_{8-10} clusters soft landed on supports were found to be highly active for the oxidative dehydrogenation of propane while maintaining a high selectivity for the formation of propylene.[59] Such "atom-by-atom" insight into the catalytic activity and selectivity of supported clusters is only possible through the preparation of well-defined samples by the soft landing of mass-selected ions.

The structural evolution of clusters on supports under reaction conditions is critical to their long-term performance, with the support playing a key role in determining stability. For example, characterization of Pd_n clusters soft landed onto TiO_2 supports revealed that deactivation proceeds through an alloy-like, strong metal–support interaction that chemically modifies the clusters through electronic interactions with the support.[60] The structural evolution of size-selected (1.4–22 nm diameter) cobalt nanoparticles during the oxidative dehydrogenation of cyclohexane was also explored.[61] Interestingly, small and intermediate-size clusters retained their morphology, while larger particles transformed into hollow spheres as a result of the nanoscale Kirkendall effect. Larger bimetallic nanoparticles containing Co and Pt were prepared on alumina supports and characterized using in situ X-ray scattering and absorption techniques to examine the evolution of their size, shape, and oxidation state under the reaction conditions.[62] The changes in the oxidation states of Co and Pt exhibited a nonlinear dependence on the Pt/Co atomic ratio of the clusters. In another study, size-dependent structural transformations (Ostwald versus Smoluchowski ripening) of Au nanoparticles during CO oxidation were explored.[63] In all of these cases, extracting interpretable information about how supports influence cluster reactivity and stability relied on the preparation of precisely defined systems by ion soft landing.

Until recently, cluster deposition experiments were performed primarily in ultrahigh vacuum under controlled conditions at low temperature and pressure. In recent years, however, there has been an evolution from performing experiments exclusively in this well-defined but idealized vacuum environment to the solution phase. For example, the activity of sub-nanometer-sized soft-landed clusters under “applied reaction conditions” has been explored.[64–65] A detrimental effect of the cluster size on the electrochemical ORR was discovered. In a related study, liquid-phase CV measurements on size-selected Pt_n clusters soft landed on glassy carbon electrodes without exposure to the ambient environment were performed by using a unique vacuum-based electrochemical cell.[65,67] This study revealed surprisingly strong effects of the cluster size, with Pt_7 clusters promoting the reduction of O_2 to H_2O, and Pt_4 clusters promoting the oxidation and degradation of the carbon support. The unusual behavior of Pt_4 clusters provides important mechanistic insight into corrosion of the carbon support—one of the major degradation modes in PEMFCs. A commercial magnetron sputter gas aggregation source was employed to prepare bare Pt_xY nanoparticles larger than 1 nm in diameter, which were found to be highly electrochemically active toward the ORR. The remarkable activity was attributed to compressive strain exerted by the core of the nanoparticles on their surfaces.[68] Recently, the in-plane multimagnetron sputtering approach[69] combined with gas aggregation was used for the preparation of PtRu alloy nanoparticles, which were shown to be electrochemically active and stable toward the ORR when deposited on glassy carbon electrodes.[70] In a following publication, the same authors described an approach that involved seeding the sputtering gas with a small amount of volatile hydrocarbons to synthesize TaC nanoparticles that surprisingly exhibited ORR activity reminiscent of precious metals such as Pt.[40]

More recently, surprisingly high and strongly size-dependent turnover numbers for the catalytic hydrogenation of *p*-chloronitrobenzene in solution were reported for size-selected Pt_n clusters soft landed on Si wafers.[71] Another study illustrated how size-selected clusters soft landed onto carbon electrodes may be used to control the morphology of lithium peroxide discharge products that form on the cathodes of lithium-oxygen batteries during electrochemical cycling.[66] Furthermore, electrochemical characterization of soft-landed clusters has been used to examine an unusual size dependence of the electrocatalytic conversion of CO_2 on Cu nanoclusters.[73] Specifically, it was observed that Cu_{20} enhances the efficiency of anodic redox processes, while Cu_5 enhances the efficiency of cathodic processes. Surfaces containing clusters prepared by ion soft landing have, until recently, been of low coverage to ensure there is limited interaction between neighboring species. Low coverage also minimizes the extent of cluster agglomeration, which is important to ensure that the system remains well-defined for catalytic testing and theoretical modeling. Nevertheless, the flux of ionization sources has increased substantially and it is now routinely possible to generate large enough ion currents (nA) to deposit multiple layers of mass-selected clusters in a realistic length of time (days).[14,15,20] It follows that, over the last few years, unexpected phenomena have started to present themselves at these high surface coverages of clusters. For example, Ostwald ripening is a well-known process by which the size distribution of clusters or nanoparticles evolves as smaller particles dissolve and the material is redeposited onto larger particles.[73] Recent experiments revealed that size-selected Pt clusters on supports exhibit remarkable intrinsic resistance to sintering under reaction conditions as a result of suppression of Ostwald ripening by elimination of its driving force (differences in the chemical potential between different-sized clusters) through size selection.[74] These findings have substantial implications for the preparation of both catalytically active and stable surfaces.[75]

The electrochemical activity of size-selected Pt clusters supported on glassy carbon electrodes for the ORR was examined as a function of cluster coverage. A pronounced increase in the O_2 reduction current was observed at a critical edge-to-edge distance that was substantially greater than what could be accounted for by the increasing cluster coverage alone.[76] This increased activity (Figure 5) was attributed to overlap of the electric double layers in solution when neighboring clusters reached a critical separation (coverage). The authors proposed that double layer overlap results in the formation of potential hot spots which serve as active sites with ideal binding strengths for both the reactants and products (Sabatier principle). The higher cluster coverages that are now obtainable also open up opportunities to characterize size-selected clusters as supported catalysts under “real” conditions of pressure and temperature.[77] One such approach involves the deposition of size-controlled clusters from a MACS source to form multilayer stacks of carbon clusters and polyvinyl pyrrolidone. The stacks are then diced without substantial damage to the clusters to create

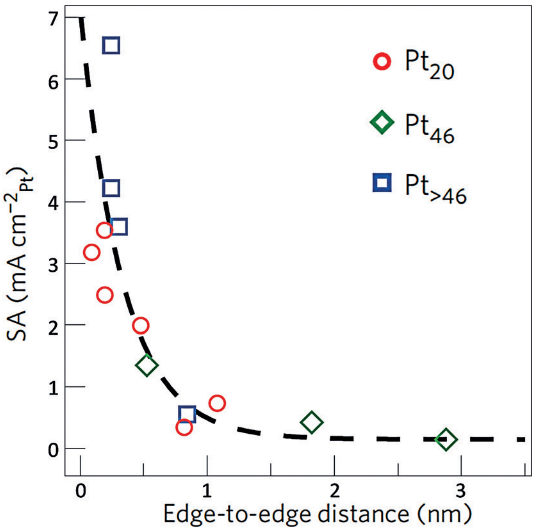

Figure 5. Plot of the O_2 reduction current as a function of the cluster–cluster distance. Reproduced from Ref. [77] with permission. Copyright 2013, Nature Publishing Group.

a catalyst powder that may be loaded into a reactor.[78] These higher coverage capabilities will, therefore, extend catalytic studies of size-selected clusters to industrially relevant conditions of temperature, pressure, and reactant flow.

7. Self-Organizing Ion-Based Layers

The deposition of large numbers of ions onto surfaces makes it possible to prepare new types of condensed-phase layers. For example, crystalline architectures of nanographenes were produced on graphite surfaces by combining matrix-assisted laser desorption ionization (MALDI) with ion soft landing.[79] Polycrystalline structures containing rodlike domains in different orientations were observed using scanning tunneling microscopy. The structures produced using ion soft landing were distinctly different from those typically formed using vacuum sublimation or solution-phase deposition. In particular, soft-landed nanographenes were found to orient perpendicular to the surface, which was attributed to the presence of charge during deposition. Subsequent self-assembly was proposed to involve neutralization and diffusion of the deposited species. In a later study, the soft landing of positively charged sodium dodecyl sulfate (SDS) species was used to produce stable multilayered molecular films (Figure 6).[80] X-ray powder diffraction and atomic force microscopy (Figure 6a–c) revealed a crystalline ordering of the films, with both upright and flat lying islands of inverse bilayers (Figure 6d) formed through self-assembly of the molecular precursors. Self-organization of these layers was found to be controlled by both molecule–surface and intermolecular interactions.

In contrast to cations that readily lose their charge on conducting surfaces, the high-coverage deposition of stable anions generates layers containing charged species that readily attract neutral molecules from the gas phase. A recent study showed that these previously unreported ion-based layers stabilized by coadsorption of gas-phase molecules can exhibit self-organization processes known as "dewetting" after exposure to ambient conditions.[41] The strong influence of the properties of the deposited anions on the self-organization process was systematically investigated using a series of highly stable and structurally similar dianions: $[B_{12}X_{12}]^{2-}$ (X = F, Cl, Br, I). An example of the observed dewetting of layers prepared by soft landing of $[B_{12}Cl_{12}]^{2-}$ and $[B_{12}I_{12}]^{2-}$ anions onto different locations of the same FSAM surface is shown in Figure 7. The two layers developed remarkably differently after exposure to air (Figure 7). In the case of the $[B_{12}Cl_{12}]^{2-}$-based layer, characteristic droplet patterns formed on the surface within one day. In contrast, the $[B_{12}I_{12}]^{2-}$-based layer remained stable for many days before developing into a colorful material over two weeks under ambient conditions. The color originates from a variety of different morphologies that scatter light and are formed by dewetting mechanisms different from the process

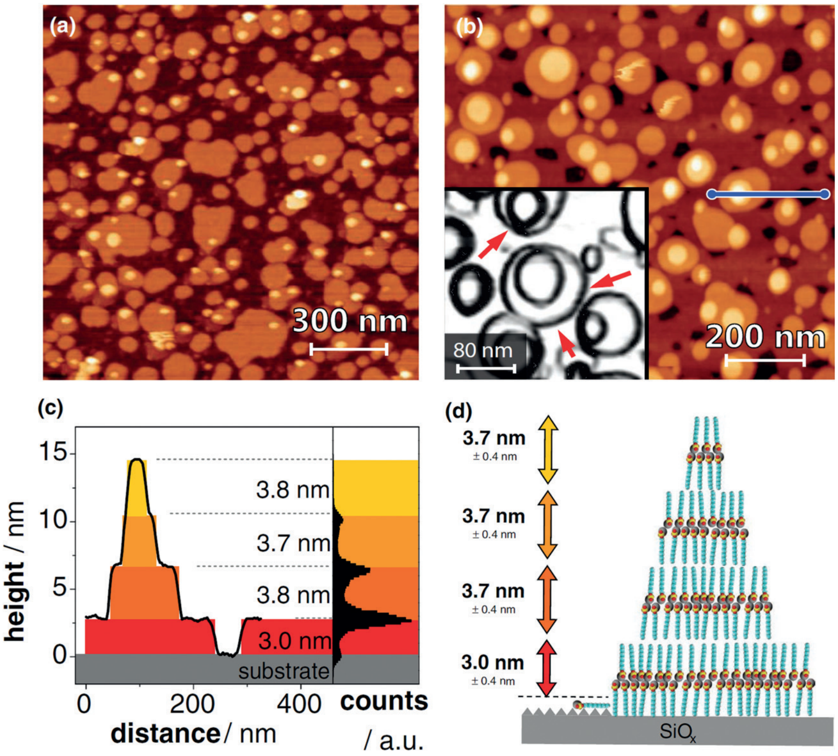

Figure 6. SDS layers on SiO_x a) AFM image at sub-monolayer coverage. b) AFM image of multilayer SDS islands; the cross-section is indicated. Inset: edge-filtered image: the red arrows indicate straight edges. c) Cross-section: first the SDS layer (3.0 nm) and then three stacked double layers (3.7–3.8 nm). The height histogram is derived from the whole AFM image (b). d) Schematic model of layer formation of SDS on SiO_x. Reproduced from Ref. [81] with permission. Copyright 2012, Wiley-VCH Verlag.

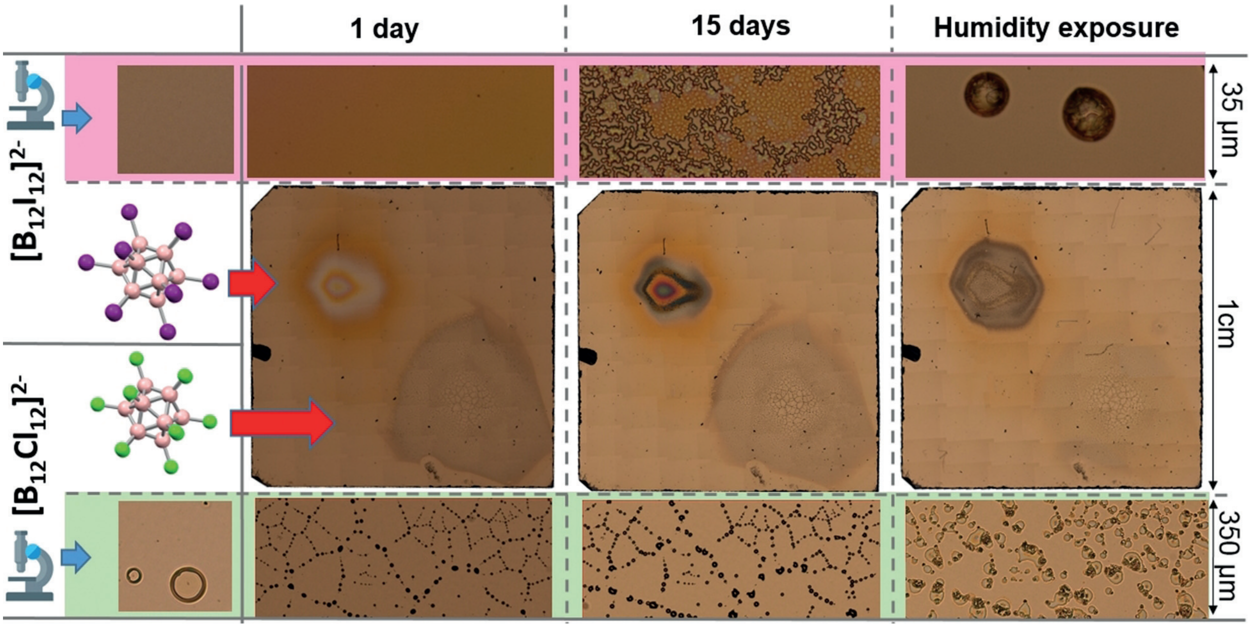

Figure 7. Optical microscope images comparing $[B_{12}Cl_{12}]^{2-}$- and $[B_{12}I_{12}]^{2-}$-based layers after exposure to ambient conditions. An overview of the surface is shown in the middle row, while light microscope images are presented in the bottom and top rows. In the case of $[B_{12}Cl_{12}]^{2-}$-based layers, holes are formed in the layers immediately upon contact with air. These holes grow and the borders merge into each other by forming rims that break and result in the shown droplet pattern.

observed for the $[B_{12}Cl_{12}]^{2-}$ layers. Droplet formation in the $[B_{12}I_{12}]^{2-}$ layer could only be promoted by subjecting the surface to wet nitrogen. In contrast, exposure of the $[B_{12}Cl_{12}]^{2-}$ layer to a large amount of water vapor resulted in the droplets completely disintegrating. This shows that the self-organizing material exposed to ambient conditions is still a metastable phase with potential for subsequent morphological transformations.

Chemical characterization of the layers revealed that, in addition to intact anions, they contain organic molecules (mostly phthalates) originating from the background of the vacuum system. X-ray photoelectron spectroscopy indicated that 2–3 organic molecules are coadsorbed per soft-landed anion. The intake of moisture into the hygroscopic layers was found to drive the self-organization process, and the dewetting mechanism was shown to be highly sensitive to the nature of the deposited anions, the coadsorbed molecules, and the underlying surface. Remarkable differences in the stability and the time frame of the dewetting were observed along the series of $[B_{12}X_{12}]^{2-}$ ($X=F$, Cl, Br, I) anions. This unexpected observation was attributed to differences in the internal charge distributions of the anions $[B_{12}X_{12}]^{2-}$. Computational population analysis methods predict a strong negative charge on the ligand shell for smaller halogens, while a slightly positive partial charge is assigned to the halogens for $X=I$.

Based on these differences between the soft-landed ions and the dramatic changes in the bulk properties of the resulting layers, it is reasonable to propose that the charge of the outer shell of the anions is a key factor in determining the stability of the anion-based layers. Specifically, a large partial negative charge on the surface of the anions with smaller halogens may lead to stronger repulsion with the negatively oriented surface dipole of the FSAM and to stronger water binding. In contrast, the partially positively charged shell of the $[B_{12}I_{12}]^{2-}$ anion may result in weaker interactions with neutral species and, therefore, a less efficient incorporation of water molecules into the layer. It follows that the intrinsic properties of the anions, often shielded by their counterions in the condensed phase, have a strong influence on the properties of high-coverage soft-landed materials.

The observed slow self-organization may be attributed to charge imbalance in the layer generated by anion accumulation, which stabilizes the layer through a strong electrostatic binding to the surface (see the capacitor model, Figure 2a). If charge balancing proceeds over time under ambient conditions, strong electrostatic interactions are replaced by weaker interfacial forces that determine the final morphology of the layer. These observations show the potential of ion soft landing for the preparation of anion-based layers for understanding the self-organization of novel materials and controlled formation of well-defined features on surfaces.

8. Biological and Soft Materials

High-flux ion deposition also has been instrumental in understanding the assembly of large floppy molecules on surfaces. For example, scanning tunneling microscopy (STM) imaging of trioctyl triazatriangulenium (TATA) deposited onto a Au(111) surface showed the formation of molecular architectures (Figure 8, top).[81] It was found that the alkyl chains of the trioctyl-TATA molecules are bent such that the adsorbed molecules are chiral. Remarkably, out of eight possible configurations of the octyl chains in the molecule, only one was observed on the surface. Soft landing of trioctyl-TATA molecules onto clean metal surfaces led to homochiral

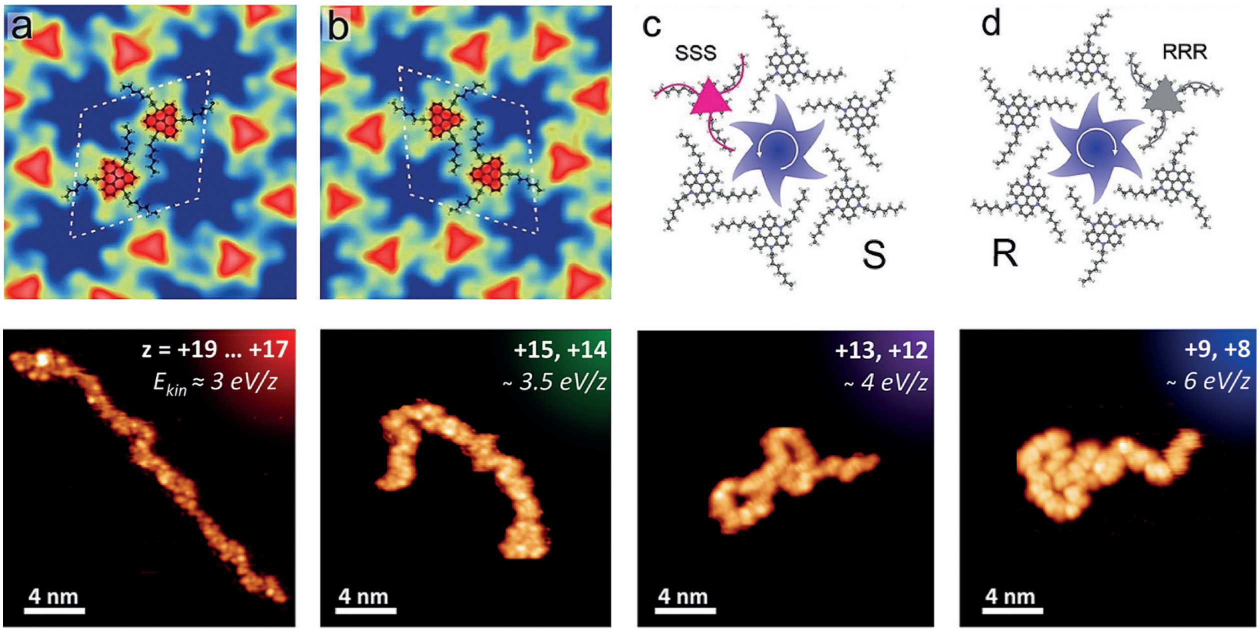

Figure 8. Top: STM images of homochiral trioctyl-TATA patterns with a) *S* and b) *R* chirality. The unit cells are shown with dashed lines. c,d) Models of the c) *S* and d) *R* arrangements. Reproduced from Ref. [82] with permission. Copyright 2015, American Chemical Society. Bottom: STM images after deposition of charge-state-filtered CytC ions on a Cu(100) surface. The charge states and kinetic energies are indicated in each panel. Reproduced from Ref. [83] with permission. Copyright 2014, American Chemical Society.

hexagonal arrangements. STM also has been used for imaging soft-landed peptides and proteins along with their formed structures on surfaces. In these studies, the charge state of the protein is commonly used to control the initial conformation (compact/extended) of the precursor ion.[82,83] The evolution of the conformation of cytochrome c on Cu(100) as a function of charge state is shown in Figure 8 (bottom).[82] As expected based on the Coulomb repulsion between the like-charged groups, more extended conformations were observed when higher charge states of the protein were selected for soft landing. The initial charge state has also been identified as an important parameter in determining the final conformations of ubiquitin ions on SAMs.[83] Furthermore, infrared spectroscopy of the soft-landed ubiquitin ions indicated that they undergo conformational changes over the course of several hours. These changes likely result from either the folding or self-assembly of the deposited species on the surfaces. Both folding and dimerization have been observed for soft-landed bradykinin ions using STM.[84] The relative yield of these processes is strongly dependent on the properties of the surface. For example, folded dimers of soft-landed bradykinin ions were the dominant species observed on Cu(100), while folded isolated molecules were observed on Cu(110).

Protein adsorption onto metal surfaces may result in substantial changes in secondary and tertiary structure. Recently, a new technique for imaging soft-landed proteins in their native conformation was introduced.[85] In this approach, proteins are soft landed onto freestanding graphene sheets and their conformation is examined using low-energy electron holography. Holography imaging of the relatively small proteins (cytochrome c, bovine serum albumin, and hemoglobin) with sub-nanometer resolution was demonstrated and the results confirmed that proteins were present in vacuum in their fully neutralized folded conformation. It has been proposed that this capability will also enable the imaging of hydrated proteins.

The covalent attachment of complex molecules to surfaces is critical to several applications, including the preparation of biosensors and protein microarrrays.[86] Previous studies demonstrated the efficient reactive landing of peptide ions onto SAMs terminated with labile functional groups[87] and carbon nanotubes.[88] Direct dynamics simulations provided important insights into the effect of the charge state and kinetic energy on the efficiency and mechanisms of reactive peptide deposition.[9,89] Good qualitative agreement between the experimental and theoretical results indicates the predictive power of direct dynamics simulations, which may be used in future studies to design ion–surface reactions for particular applications. Recent experimental studies examined the reactive landing of multifunctional molecules. For example, the deposition of different generations of dendrimer ions onto SAMs enabled a systematic study of the effect of the number of functional groups in a complex projectile ion on the efficiency of forming covalent bonds with the surface.[90] It was demonstrated that the reactive landing efficiency increases in proportion to the number of exposed reactive groups in the ion. In a related study, this observation was extended to peptides and proteins.[91] In contrast to dendrimers, which showed no measurable effect of the charge state of the ion on the binding efficiency, more efficient bond formation was observed for the higher charge state of ubiquitin, which has an extended conformation. This finding was attributed to the larger number of reactive groups on the surface of the extended conformation.

9. Summary and Outlook

Ion soft landing has a productive history in the preparation of low-coverage samples on surfaces for fundamental studies in catalysis, surface science, and chemical analysis. Recent advances in instrumentation, including electrospray ionization, magnetron sputtering, the electrodynamic ion funnel, and the matrix assembly cluster source, now allow much larger fluxes of mass-selected ions to be delivered routinely to surfaces. In addition, nonthermal ionization methods as well as gas-phase techniques, such as collision-induced dissociation and ion–molecule reactions, are being exploited to generate new materials that cannot be synthesized by condensed-phase methods. At the same time, more accessible instrumentation has been developed that enables some of the advantages of soft landing in vacuum to be achieved on the laboratory benchtop under ambient conditions. Rapidly desolvating droplets offer a new medium for exploring and promoting reactions at interfaces. It is the higher ion fluxes, however, that are revealing unexpected new phenomena, including emergent catalytic hot spots at critical cluster coverages and the formation of macroscopic films with behavior that may be controlled through the intrinsic properties of the gas-phase ions. The surprising accumulation of such large quantities of like-charged ions on surfaces may be explained using a capacitor model that balances the charge of the ions with that of an induced mirror potential in the underlying conductive substrate. Other processes that may control the self-organization of ion-based layers should be explored in future studies. For example, exposing the layers to an energetic electron beam may be used for the direct writing of well-defined nanoscale features for potential applications in photonics and nanoscale patterning. Importantly, the properties of isolated ions, extensively investigated in mass spectrometry experiments in the gas phase, may be used to rationalize the design of new layered materials with previously unreported properties. However, the molecular control demonstrated over these layers can only be fully exploited by obtaining a physical understanding of their internal structure. Dewetting mechanisms, which have been extensively investigated by the physics community, provide important insights into the properties of these novel materials.

Although it is unlikely that ion soft landing will be able to produce gram quantities of high-purity molecular building blocks for materials synthesis, we anticipate that it will complement the capabilities of well-established techniques for the preparation of high-quality thin layers on substrates, such as molecular beam epitaxy and atomic layer deposition. In particular, the capabilities of these techniques in some advanced commercial applications will be expanded to include ionic building blocks and large, low-volatility molecules. Current vacuum-based ion soft landing instrumentation generates ion currents of up to 8 nA, which results in the deposition of a monolayer over an area of 1 cm^2 in less than an hour. Space–charge effects may present a challenge to obtaining substantially higher ion currents (microamps) under vacuum conditions. Clever approaches developed for high-energy physics experiments, including counter-propagating ion beams of opposite charge and the introduction of ionizable background gases, may help surmount space–charge limitations. Furthermore, soft landing under ambient conditions may help alleviate some of the challenges associated with deposition from higher ion fluxes and provide a practical alternative for scaling up the deposition process. These advances will allow ion soft landing to transition from the realm of fundamental science using monolayers to the preparation of 3D functional materials for incorporation into macroscopic devices such as capacitors, batteries, and photovoltaic systems. High-flux ion beams may also be patterned using templates, masks, or alternating electric fields, which direct ions towards specific spots on substrates. This approach may be used to prepare surfaces with well-defined active sites for applications in catalysis, energy conversion and storage, and sensing.

Acknowledgements

We acknowledge long-term support of the ion soft landing research from the U.S. Department of Energy (DOE), Office of Science, Office of Basic Energy Sciences, Division of Chemical Sciences, Geosciences and Biosciences. J.W. acknowledges a Feodor Lynen Fellowship from the Alexander von Humboldt Foundation and support from the Pacific Northwest National Laboratory (PNNL) through the Alternate Sponsored Fellow Program. A portion of the research described in this Review was performed using EMSL, a DOE Office of Science User Facility sponsored by the Office of Biological and Environmental Research. PNNL is a multiprogram national laboratory operated for the DOE by Battelle.

Conflict of interest

The authors declare no conflict of interest.

How to cite: *Angew. Chem. Int. Ed.* **2018**, *57*, 16270–16284
Angew. Chem. **2018**, *130*, 16506–16521

[1] V. Grill, J. Shen, C. Evans, R. G. Cooks, *Rev. Sci. Instrum.* **2001**, *72*, 3149–3179.

[2] B. Gologan, J. M. Wiseman, R. G. Cooks, in *Principles of Mass Spectrometry Applied to Biomolecules* (Eds.: J. Laskin, C. Lifshitz), Wiley, Hoboken, **2006**.

[3] J. Laskin, P. Wang, O. Hadjar, *Phys. Chem. Chem. Phys.* **2008**, *10*, 1079–1090.

[4] G. E. Johnson, Q. C. Hu, J. Laskin, *Annu. Rev. Anal. Chem.* **2011**, *4*, 83–104.

[5] J. Cyriac, T. Pradeep, H. Kang, R. Souda, R. G. Cooks, *Chem. Rev.* **2012**, *112*, 5356–5411.

[6] G. Verbeck, W. Hoffmann, B. Walton, *Analyst* **2012**, *137*, 4393–4407.

[7] G. E. Johnson, D. Gunaratne, J. Laskin, *Mass Spectrom. Rev.* **2016**, *35*, 439–479.

[8] J. Laskin, G. E. Johnson, V. Prabhakaran, *J. Phys. Chem. C* **2016**, *120*, 23305–23322.

[9] S. Pratihar, G. L. Barnes, J. Laskin, W. L. Hase, *J. Phys. Chem. Lett.* **2016**, *7*, 3142–3150.

[10] S. Rauschenbach, M. Ternes, L. Harnau, K. Kern, in *Annu. Rev. Anal. Chem.* **2016**, 473–498.

[11] V. Franchetti, B. H. Solka, W. E. Baitinger, J. W. Amy, R. G. Cooks, *Int. J. Mass Spectrom. Ion Processes* **1977**, *23*, 29–35.

[12] Z. Ouyang, Z. Takats, T. A. Blake, B. Gologan, A. J. Guymon, J. M. Wiseman, J. C. Oliver, V. J. Davisson, R. G. Cooks, *Science* **2003**, *301*, 1351–1354.

[13] H. Haberland, M. Karrais, M. Mall, *Z. Phys. D* **1991**, *20*, 413–415.

[14] K. D. Gunaratne, V. Prabhakaran, Y. M. Ibrahim, R. V. Norheim, G. E. Johnson, J. Laskin, *Analyst* **2015**, *140*, 2957–2963.

[15] M. Pauly, M. Sroka, J. Reiss, G. Rinke, A. Albarghash, R. Vogelgesang, H. Hahne, B. Kuster, J. Sesterhenn, K. Kern, S. Rauschenbach, *Analyst* **2014**, *139*, 1856–1867.

[16] L. Martínez, M. Díaz, E. Roman, M. Ruano, D. Llamosa, Y. Huttel, *Langmuir* **2012**, *28*, 11241–11249.

[17] F. Caruso, A. Bellacicca, P. Milani, *Appl. Phys. Lett.* **2016**, *108*, 163501.

[18] C. H. Zhang, H. Tsunoyama, H. Akatsuka, H. Sekiya, T. Nagase, A. Nakajima, *J. Phys. Chem. A* **2013**, *117*, 10211–10217.

[19] P. R. Ellis, C. M. Brown, P. T. Bishop, J. Yin, K. Cooke, W. D. Terry, J. Liu, F. Yin, R. E. Palmer, *Faraday Discuss.* **2016**, *188*, 39–56.

[20] R. E. Palmer, L. Cao, F. Yin, *Rev. Sci. Instrum.* **2016**, *87*, 046103.

[21] R. Cai, N. Jian, S. Murphy, K. Bauer, R. E. Palmer, *APL Materials* **2017**, *5*, 053405.

[22] A. K. Badu-Tawiah, C. P. Wu, R. G. Cooks, *Anal. Chem.* **2011**, *83*, 2648–2654.

[23] M. Wleklinski, D. Sarkar, A. Hollerbach, T. Pradeep, R. G. Cooks, *Phys. Chem. Chem. Phys.* **2015**, *17*, 18364–18373.

[24] A. Y. Li, Z. Baird, S. Bag, D. Sarkar, A. Prabhath, T. Pradeep, R. G. Cooks, *Angew. Chem. Int. Ed.* **2014**, *53*, 12528–12531; *Angew. Chem.* **2014**, *126*, 12736–12739.

[25] J. Hou, Q. N. Zheng, A. K. Badu-Tawiah, C. Q. Xiong, C. Z. Guan, S. M. Chen, Z. X. Nie, D. Wang, L. J. Wan, *Chem. Commun.* **2016**, *52*, 13660–13663.

[26] H. R. Fang, D. Wang, L. Yuan, X. F. Wu, H. P. Guo, H. W. Chen, K. Huang, S. H. Feng, *New J. Chem.* **2017**, *41*, 2878–2882.

[27] P. Pompach, O. Benada, M. Rosulek, P. Darebna, J. Hausner, V. Ruzicka, M. Volny, P. Novak, *Anal. Chem.* **2016**, *88*, 8526–8534.

[28] Z. Baird, P. Wei, R. G. Cooks, *Analyst* **2015**, *140*, 696–700.

[29] P. A. Kottke, J. Y. Lee, A. P. Jonke, C. A. Seneviratne, E. S. Hecht, D. C. Muddiman, M. P. Torres, A. G. Fedorov, *Anal. Chem.* **2017**, *89*, 8981–8987.

[30] Q. He, A. K. Badu-Tawiah, S. M. Chen, C. Q. Xiong, H. H. Liu, Y. M. Zhou, J. Hou, N. Zhang, Y. F. Li, X. B. Xie, J. N. Wang, L. Q. Mao, Z. X. Nie, *Anal. Chem.* **2015**, *87*, 3144–3148.

[31] A. K. Badu-Tawiah, D. I. Campbell, R. G. Cooks, *J. Am. Soc. Mass Spectrom.* **2012**, *23*, 1077–1084.

[32] A. K. Badu-Tawiah, J. Cyriac, R. G. Cooks, *J. Am. Soc. Mass Spectrom.* **2012**, *23*, 842–849.

[33] S. A. Miller, H. Luo, S. J. Pachuta, R. G. Cooks, *Science* **1997**, *275*, 1447–1450.

[34] O. Hadjar, J. H. Futrell, J. Laskin, *J. Phys. Chem. C* **2007**, *111*, 18220–18225.

[35] J. Laskin, P. Wang, O. Hadjar, J. H. Futrell, J. Alvarez, R. G. Cooks, *Int. J. Mass Spectrom.* **2007**, *265*, 237–243.

[36] K. D. D. Gunaratne, G. E. Johnson, A. Andersen, D. Du, W. Y. Zhang, V. Prabhakaran, Y. H. Lin, J. Laskin, *J. Phys. Chem. C* **2014**, *118*, 27611–27622.

[37] K. D. D. Gunaratne, V. Prabhakaran, A. Andersen, G. E. Johnson, J. Laskin, *Phys. Chem. Chem. Phys.* **2016**, *18*, 9021–9028.

[38] G. E. Johnson, T. Priest, J. Laskin, *ACS Nano* **2012**, *6*, 573–582.

[39] G. E. Johnson, T. Priest, J. Laskin, *J. Phys. Chem. C* **2012**, *116*, 24977–24986.

[40] G. E. Johnson, T. Moser, M. Engelhard, N. D. Browning, J. Laskin, *J. Chem. Phys.* **2016**, *145*, 174701.

[41] J. Warneke, M. E. McBriarty, S. L. Riechers, S. China, M. H. Engelhard, E. Aprà, R. P. Young, N. M. Washton, C. Jenne, G. E. Johnson, J. Laskin, *Nat. Commun.* **2018**, *9*, 1889.

[42] A. J. Bard, H. D. Abruna, C. E. Chidsey, L. R. Faulkner, S. W. Feldberg, K. Itaya, M. Majda, O. Melroy, R. W. Murray, *J. Phys. Chem.* **1993**, *97*, 7147–7173.

[43] S. Srinivasan, in *Fuel Cells: From Fundamentals to Applications* (Ed.: S. Srinivasan), Springer, Boston, **2006**, pp. 27–92.

[44] M. Favaro, B. Jeong, P. N. Ross, J. Yano, Z. Hussain, Z. Liu, E. J. Crumlin, *Nat. Commun.* **2016**, *7*, 12695.

[45] P. K. Shen, C.-Y. Wang, S. P. Jiang, X. Sun, J. Zhang, *Electrochemical Energy: Advanced Materials and Technologies*, CRC Press, Boca Raton, FL, **2015**.

[46] A. J. Bard, L. R. Faulkner, *Electrochemical Methods: Fundamentals and Applications*, 2nd ed., Wiley, Hoboken, **2000**.

[47] V. Prabhakaran, B. L. Mehdi, J. J. Ditto, M. H. Engelhard, B. Wang, K. D. D. Gunaratne, D. C. Johnson, N. D. Browning, G. E. Johnson, J. Laskin, *Nat. Commun.* **2016**, *7*, 11399.

[48] A. McInnes, S. R. Plant, I. M. Ornelas, R. E. Palmer, K. G. U. Wijayantha, *Sustainable Energy Fuels* **2017**, *1*, 336–344.

[49] V. Prabhakaran, G. E. Johnson, B. Wang, J. Laskin, *Proc. Natl. Acad. Sci. USA* **2016**, *113*, 13324–13329.

[50] P. Fayet, F. Granzer, G. Hegenbart, E. Moisar, B. Pischel, L. Woste, *Phys. Rev. Lett.* **1985**, *55*, 3002–3004.

[51] D. M. Cox, W. Eberhardt, P. Fayet, Z. Fu, B. Kessler, R. D. Sherwood, D. Sondericker, A. Kaldor, *Z. Phys. D* **1991**, *20*, 385–386.

[52] V. N. Popok, I. Barke, E. E. B. Campbell, K. H. Meiwes-Broer, *Surf. Sci. Rep.* **2011**, *66*, 347–377.

[53] E. C. Tyo, S. Vajda, *Nat. Nanotechnol.* **2015**, *10*, 577–588.

[54] S. Vajda, M. G. White, *ACS Catal.* **2015**, *5*, 7152–7176.

[55] U. Heiz, F. Vanolli, L. Trento, W. D. Schneider, *Rev. Sci. Instrum.* **1997**, *68*, 1986–1994.

[56] B. Yoon, H. Hakkinen, U. Landman, A. S. Worz, J. M. Antonietti, S. Abbet, K. Judai, U. Heiz, *Science* **2005**, *307*, 403–407.

[57] W. E. Kaden, T. P. Wu, W. A. Kunkel, S. L. Anderson, *Science* **2009**, *326*, 826–829.

[58] V. Habibpour, C. R. Yin, G. Kwon, S. Vajda, R. E. Palmer, *J. Exp. Nanosci.* **2013**, *8*, 993–1003.

[59] S. Vajda, M. J. Pellin, J. P. Greeley, C. L. Marshall, L. A. Curtiss, G. A. Ballentine, J. W. Elam, S. Catillon-Mucherie, P. C. Redfern, F. Mehmood, P. Zapol, *Nat. Mater.* **2009**, *8*, 213–216.

[60] W. E. Kaden, W. A. Kunkel, F. S. Roberts, M. Kane, S. L. Anderson, *Surf. Sci.* **2014**, *621*, 40–50.

[61] S. Bartling, C. R. Yin, I. Barke, K. Oldenburg, H. Hartmann, V. von Oeynhausen, M. M. Pohl, K. Houben, E. C. Tyo, S. Seifert, P. Lievens, K. H. Meiwes-Broer, S. Vajda, *ACS Nano* **2015**, *9*, 5984–5998.

[62] B. Yang, G. Khadra, J. Tuaillon-Combes, E. C. Tyo, M. J. Pellin, B. Reinhart, S. Seifert, X. Q. Chen, V. Dupuis, S. Vajda, *J. Phys. Chem. C* **2016**, *120*, 21496–21504.

[63] K. J. Hu, S. R. Plant, P. R. Ellis, C. M. Brown, P. T. Bishop, R. E. Palmer, *J. Am. Chem. Soc.* **2015**, *137*, 15161–15168.

[64] S. Kunz, K. Hartl, M. Nesselberger, F. F. Schweinberger, G. Kwon, M. Hanzlik, K. J. J. Mayrhofer, U. Heiz, M. Arenz, *Phys. Chem. Chem. Phys.* **2010**, *12*, 10288–10291.

[65] A. von Weber, S. L. Anderson, *Acc. Chem. Res.* **2016**, *49*, 2632–2639.

[66] J. Lu, L. Cheng, K. C. Lau, E. Tyo, X. Y. Luo, J. G. Wen, D. Miller, R. S. Assary, H. H. Wang, P. Redfern, H. M. Wu, J. B. Park, Y. K. Sun, S. Vajda, K. Amine, L. A. Curtiss, *Nat. Commun.* **2014**, *5*, 4895.

[67] S. Proch, M. Wirth, H. S. White, S. L. Anderson, *J. Am. Chem. Soc.* **2013**, *135*, 3073–3086.

[68] P. Hernandez-Fernandez, F. Masini, D. N. McCarthy, C. E. Strebel, D. Friebel, D. Deiana, P. Malacrida, A. Nierhoff, A.

Bodin, A. M. Wise, J. H. Nielsen, T. W. Hansen, A. Nilsson, I. E. L. Stephens, I. Chorkendorff, *Nat. Chem.* **2014**, *6*, 732 – 738.
[69] G. E. Johnson, R. Colby, J. Laskin, *Nanoscale* **2015**, *7*, 3491 – 3503.
[70] G. E. Johnson, R. Colby, M. Engelhard, D. Moon, J. Laskin, *Nanoscale* **2015**, *7*, 12379 – 12391.
[71] M. Rondelli, G. Zwaschka, M. Krause, M. D. Rotzer, M. N. Hedhili, M. P. Hoger, V. D'Elia, F. F. Schweinberger, J. M. Basset, U. Heiz, *ACS Catal.* **2017**, *7*, 4152 – 4162.
[72] R. Passalacqua, S. Parathoner, G. Centi, A. Halder, E. C. Tyo, B. Yang, S. Seifert, S. Vajda, *Catal. Sci. Technol.* **2016**, *6*, 6977 – 6985.
[73] P. W. Voorhees, *J. Stat. Phys.* **1985**, *38*, 231 – 252.
[74] K. Wettergren, F. F. Schweinberger, D. Deiana, C. J. Ridge, A. S. Crampton, M. D. Rotzer, T. W. Hansen, V. P. Zhdanov, U. Heiz, C. Langhammer, *Nano Lett.* **2014**, *14*, 5803 – 5809.
[75] F. R. Negreiros, A. Halder, C. R. Yin, A. Singh, G. Barcaro, L. Sementa, E. C. Tyo, M. J. Pellin, S. Bartling, K. H. Meiwes-Broer, S. Seifert, P. Sen, S. Nigam, C. Majumder, N. Fukui, H. Yasumatsu, S. Vajda, A. Fortunelli, *Angew. Chem. Int. Ed.* **2018**, *57*, 1209 – 1213; *Angew. Chem.* **2018**, *130*, 1223 – 1227.
[76] M. Nesselberger, M. Roefzaad, R. F. Hamou, P. U. Biedermann, F. F. Schweinberger, S. Kunz, K. Schloegl, G. K. H. Wiberg, S. Ashton, U. Heiz, K. J. J. Mayrhofer, M. Arenz, *Nat. Mater.* **2013**, *12*, 919 – 924.
[77] P. R. Ellis, C. M. Brown, P. T. Bishop, J. L. Yin, K. Cooke, W. D. Terry, J. Liu, F. Yin, R. E. Palmer, *Faraday Discuss.* **2016**, *188*, 39 – 56.
[78] N. Jian, K. Bauer, R. E. Palmer, *Nanotechnology* **2017**, *28*, 325601.
[79] H. J. Räder, A. Rouhanipour, A. M. Talarico, V. Palermo, P. Samorì, K. Müllen, *Nat. Mater.* **2006**, *5*, 276.
[80] S. Rauschenbach, G. Rinke, N. Malinowski, R. T. Weitz, R. Dinnebier, N. Thontasen, Z. T. Deng, T. Lutz, P. Rollo, G. Costantini, L. Harnau, K. Kern, *Adv. Mater.* **2012**, *24*, 2761 – 2767.
[81] N. Hauptmann, K. Scheil, T. G. Gopakumar, F. L. Otte, C. Schütt, R. Herges, R. Berndt, *J. Am. Chem. Soc.* **2013**, *135*, 8814 – 8817.
[82] G. Rinke, S. Rauschenbach, L. Harnau, A. Albarghash, M. Pauly, K. Kern, *Nano Lett.* **2014**, *14*, 5609 – 5615.
[83] Q. C. Hu, J. Laskin, *J. Phys. Chem. B* **2016**, *120*, 4927 – 4936.
[84] S. Rauschenbach, G. Rinke, R. Gutzler, S. Abb, A. Albarghash, D. Le, T. S. Rahman, M. Durr, L. Harnau, K. Kern, *ACS Nano* **2017**, *11*, 2420 – 2427.
[85] J. N. Longchamp, S. Rauschenbach, S. Abb, C. Escher, T. Latychevskaia, K. Kern, H. W. Fink, *Proc. Natl. Acad. Sci. USA* **2017**, *114*, 1474 – 1479.
[86] P. Wang, J. Laskin, in *Ion Beams in Nanoscience and Technology* (Eds.: R. Hellborg, H. J. Whitlow, Y. Zhang), Springer, Berlin, Heidelberg, **2009**, pp. 37 – 65.
[87] P. Wang, O. Hadjar, P. L. Gassman, J. Laskin, *Phys. Chem. Chem. Phys.* **2008**, *10*, 1512 – 1522.
[88] F. Mazzei, G. Favero, M. Frasconi, A. Tata, F. Pepi, *Chem. Eur. J.* **2009**, *15*, 7359 – 7367.
[89] G. L. Barnes, A. Podczerwinski, *J. Phys. Chem. C* **2017**, *121*, 14628 – 14635.
[90] Q. Hu, J. Laskin, *J. Phys. Chem. C* **2014**, *118*, 2602 – 2608.
[91] J. Laskin, Q. Hu, *J. Am. Soc. Mass Spectrom.* **2017**, *28*, 1304 – 1312.

Manuscript received: January 24, 2018
Accepted manuscript online: May 14, 2018
Version of record online: November 8, 2018